Nationaal Lucht- en Ruimtevaartlaboratorium
National Aerospace Laboratory NLR

NLR-TP-2001-342

Analysis of residual strength of stiffened panels with multiple site damage

M.F.J. Koolloos, H.J. ten Hoeve, F.P. Grooteman
and A.U. de Koning

Nationaal Lucht- en Ruimtevaartlaboratorium
National Aerospace Laboratory NLR

NLR-TP-2001-342

Analysis of residual strength of stiffened panels with multiple site damage

M.F.J. Koolloos, H.J. ten Hoeve, F.P. Grooteman
and A.U. de Koning

This report is based on a presentation held at the 5th Joint NASA/FAA/DoD Conference on Aging Aircraft, HYATT-Orlando, Kissimmee, Florida, USA, 10-13 September 2001.

This investigation has been carried out as part of the NLR's Basic Research Programme, workplan number S.1.B.3.

Division:	Structures and Materials
Issued:	July 2001
Classification of title:	Unclassified

Contents

NOMENCLATURE

2a	total actual crack length
$2a_e$	total fictitious crack length
$2a_0$	total crack length of leading crack
$2a_{MSD}$	total crack length of MSD crack
COD	Crack Opening Displacement
CTOD	Crack Tip Opening Displacement
d_{MSD}	centre-to-centre distance between leading crack and first MSD crack
DoD	Department of Defence
E	Young's modulus
F	rivet force
FAA	Federal Aviation Administration
G	crack driving force (strain energy release rate)
GM	coefficient matrix for crack surface load
H	panel height
J	J-integral
lig1	tip-to-tip distance between leading crack and first MSD crack
lig2	tip-to-tip distance between MSD cracks
MSD	Multiple Site Damage
NASA	National Aeronautics and Space Administration
NIST	National Institute of Standards and Technology
p(x)	stress distribution along x-axis
R	crack resistance
2s	stiffener spacing
s_{MSD}	centre-to-centre distance between MSD cracks
sl	stretch of element
t	panel thickness
UTS	ultimate tensile stress
v	displacements in y-direction
v_a	displacement in cracked sheet due to remote stress
v_b	displacement in (uncracked) sheet due to sheet-stiffener interaction forces
v_c	displacement in cracked sheet due to stress distribution p(x) along crack edge
v_s	coefficient vector for remote load
2W	total panel width
x,y	coordinates in plane of sheet parallel and normal to crack, respectively

α_1,α_2	material parameters accounting for the constraint to simulate 2- and 3-dimensional effects in the stress field surrounding the crack tip
σ_R	stress remote from crack
σ	element stress
σ_{yld}, σ_{YS}	0.2 percent offset yield strength
σ_Y	flow stress

Subscripts

sh	sheet
st	stiffener
riv	rivet

Analysis of Residual Strength of Stiffened Panels with Multiple Site Damage

M.F.J. Koolloos, H.J. ten Hoeve, F.P. Grooteman and A.U. de Koning
National Aerospace Laboratory NLR, P.O. Box 153, 8300 AD Emmeloord, The Netherlands

SUMMARY

Multiple Site Damage (MSD) is a typical problem for ageing civil and transport aircraft, where the large number of fuselage pressure cycles may cause fatigue cracking at multiple rivet locations. The residual strength of a panel with a leading crack and MSD cracks is lower than that of a panel with the same leading crack but without MSD. This paper presents an advanced engineering model to predict link-up and the residual strength in flat unstiffened and stiffened panels with one leading crack and MSD cracks. The model is verified using experimental data from the open literature: the predictions are in good agreement with the measured residual strengths.

INTRODUCTION

The Aloha accident in 1988 resulted in much attention being paid to the multiple site damage (MSD) phenomenon of riveted lap joints in aircraft fuselages. MSD is a typical problem for ageing aircraft, where the large number of fuselage pressure cycles may cause fatigue cracking at multiple rivet locations in lap joints. After some growth of the MSD cracks they may interact and crack link-up may occur, resulting in one leading crack flanked by MSD cracks[1,2].

MSD reduces the overall structural integrity. Consequently, the residual strength of a panel with a leading crack and MSD cracks is known to be lower than that of a panel with the same leading crack but without MSD[2]. In recent years research projects have been carried out to assess the residual strength of flat stiffened panels with a leading crack and MSD cracks. Tests have been done on flat panels (stiffened and unstiffened) with a leading crack and MSD cracks[3-7], and models have been developed to predict link-up of the MSD cracks and the residual strength of a panel with MSD[5-8]. The main differences between the models arise from the definitions and criteria for crack growth and link-up. Verification of the models is done with experimental data available from the open literature. At NLR a model to predict link-up and the residual strength in flat unstiffened and stiffened panels in the presence of multiple site damage has been developed. The main objective is an engineering tool that can be used in the design of aircraft. The model is based on the Strip Yield model (as implemented in the NASGRO software) for the calculation of the value of the J-integral at all crack tips and is also based on the R-curve approach. The influence of stiffeners is modelled using the displacement compatibility method.

This paper presents the NLR model and its verification. First the Strip Yield model is introduced, after which the residual strength model and the displacement compatibility method are described. Finally the model is verified based on experimental data from three institutes.

STRIP YIELD MODEL

Model Description

The Strip Yield model uses a method first proposed by Dugdale[9] to calculate the stresses and deformations around a loaded crack by considering the material to act as a series of elements behaving in a rigid plastic manner. For a thin strip lying along, but being larger in size than, the fictitious crack length, *i.e.* the actual crack and the plastic zone ahead of the crack tip, the following conditions are assumed:

1. All plastic deformation is confined within an infinitely thin strip located along the crack line.
2. Material within the strip behaves in a rigid plastic manner while material outside the strip is perfectly elastic.
3. The material in the strip is able to undergo an arbitrary stretch in the tensile direction when the stress exceeds the local yield stress, both in tension and compression.

In an application of the Strip Yield model the stresses and deformations are solved using numerical methods. The crack and the plastic zone ahead of the crack are divided into a number of finite width elements. Each element carries a constant stress across its width or a point force acting at its centre (depending on the method used to calculate the influence functions).

An element in the plastic zone can carry a stress up to the local yield limit in tension or compression. Elements on the crack surface can carry compressive stresses up to the local yield limit in compression. The displacements of all elements is determined by a contribution from the remote load σ_R and from the element stresses $\sigma(x)$. This is illustrated in figure 1. The basic solutions for these displacements are obtained from the Westergaard solutions[10] for the two loading conditions, yielding the following expression for the total displacement at element i:

$$v(i) = v_s(i)\sigma_R + GM(i, j)\sigma(j) \tag{1}$$

where ν_s and GM are the coefficient vector and matrix for the remote load and crack surface load respectively, and $\sigma(j)$ is the stress in element j. It must be noted here that for the present model GM can be solved for panels of infinite and finite width.

The deformations in the plastic area ahead of the crack tip are determined as follows. Since the material behaves in a rigid plastic manner, elements loaded to the yield limit can undergo an arbitrary stretch, referred to as *sl*. The stretch of these elements is dictated by the elastic surrounding of the plastic area. Consider a point in the elastic area just above an element that is yielding in tension as the result of a remote load. This point is connected to the midplane (plane of the crack) via the yielding element and is displaced over a distance *v(i)*, see Eq. (1) The crack opening displacement of all elements in the plastic zone is zero. In other words: the conditions for the plastic zone are:

$$sl(i) = v(i) \tag{2}$$

$$COD(i) = 0 \tag{3}$$

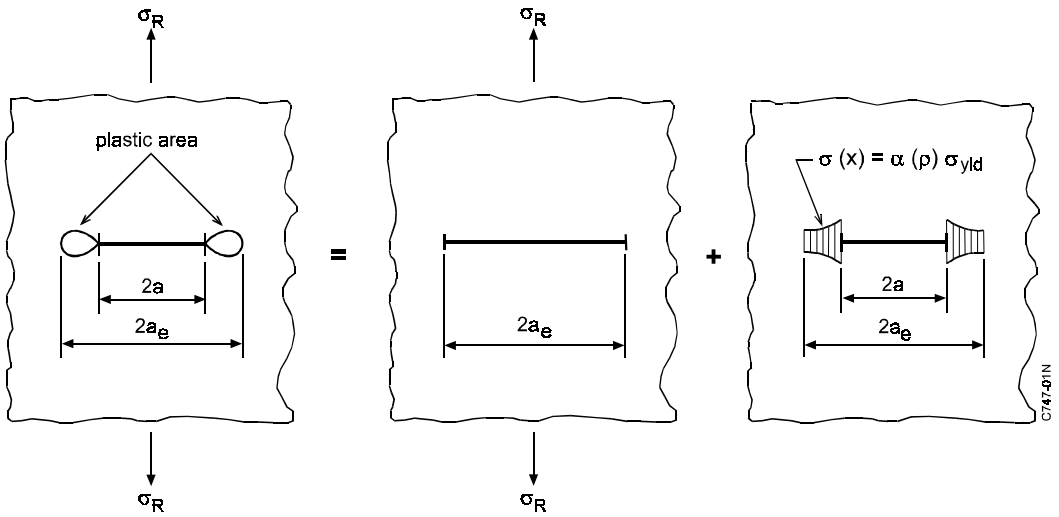

Figure 1 *The fictitious crack length ($2a_e$) and load cases used in the Strip Yield model*

In the cracked area the crack opening displacement is equal to the calculated *v(i)* minus the stretch left in the element. This stretch is the result of loads applied to the structure when this element is part of the plastic zone. If the calculated *v(i)* is less than the stretch left in the element the crack is closed. The crack opening displacement is set to zero and the stretch is set to *v(i)*. This results in the following relations for the open part of the crack:

$$COD(i) = v(i) - sl(i) \tag{4}$$

$$sl(i) = sl(i) \tag{5}$$

and:

$$COD(i) = 0 \tag{6}$$

$$sl(i) = v(i) \tag{7}$$

for the part of the crack which is closed.

From these equations the element stresses, crack opening displacements and stretches can be solved taking into account the following boundary conditions for the stresses:

$$\alpha_1 \sigma_{yld} \le \sigma(i) \le \alpha_2 \sigma_{yld} \tag{8}$$

$$\alpha_1 \sigma_{yld} < \sigma(i) \le 0 \tag{9}$$

in the closed part of the crack, and

$$\sigma(i) = 0 \tag{10}$$

in the open part of the crack. In these equations σ_{yld} is the uniaxial yield limit of the material, and α_1 and α_2 are material parameters accounting for the constraint to simulate 2- and 3-dimensional effects in the stress field surrounding the crack tip. Eqs. (1)-(10) are solved iteratively using the Gauss-Seidel solution procedure.

J-integral

Since the plastic zone near a crack tip cannot be considered negligibly small, the strain energy release rate, G, is obtained from the J-integral. For the Strip Yield model it has been shown that there exists a simple relation between the J-integral and the crack tip opening displacement (CTOD)[11,12]. The CTOD is a somewhat artificial mathematical quantity that cannot be verified experimentally. The relation between J and CTOD is:

$$J = \sigma_{yld}\ CTOD \tag{11}$$

The stretches at the element centres are one set of quantities obtained from a solution of the Strip Yield model. The CTOD can be calculated from the stretches of the first two elements in the plastic zone (the ones just ahead of the crack tip). From this crack tip opening displacement the J-integral is calculated according to the relation given above.

Multiple Site Damage

In the case of multiple site damage the series of collinear cracks can be modelled as the superposition of known cases as shown in figure 2. A surface load has to be applied to the ligaments between the cracks in order to close the crack locally. The stresses required to fulfil this condition are bounded by the yield stress. These stresses are obtained directly from the Strip Yield model if it is solved with the boundary conditions given in Eqs. (6) and (7) applied to the ligaments between the cracks and the plastic zones outside the outer crack tips. From this solution the opening stress and the J-integral can be calculated for all tips. In addition, for small scale yielding conditions the stress intensity factors can be calculated from the CTODs.

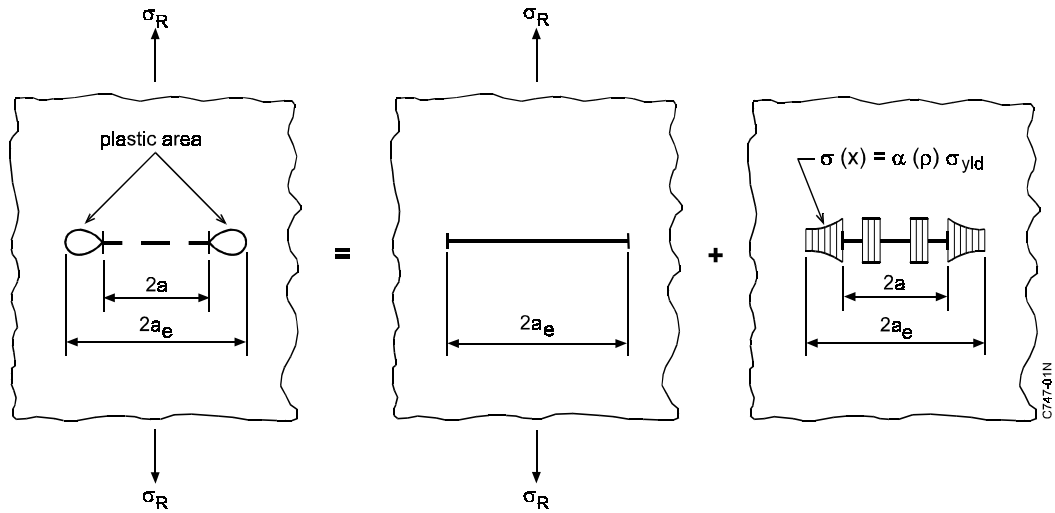

Figure 2 *The fictitious crack length ($2a_e$) and load cases used in the Strip Yield model for MSD*

RESIDUAL STRENGTH MODEL

Unstiffened Panels

The residual strength of a structure can be calculated by solving the following equations[12]:

$$G = R \tag{12}$$

$$\frac{\partial G}{\partial a} = \frac{\partial R}{\partial a} \tag{13}$$

where R is a material characteristic given in the form of a table or an expression, and G is obtained from the Strip Yield model. For simple geometries (like a centre cracked infinite sheet) there exists an explicit relation for G and R and for $\partial G/\partial a$ and $\partial R/\partial a$. In these cases Eqs. (12) and (13) can be solved directly. In case the Strip Yield model is used to calculate G for multiple collinear cracks (MSD) there is not a simple relation between G and a. The derivative of G with respect to a has to be solved numerically to be able to solve Eqs. (12) and (13).

Alternatively the following method can be used: Assume a remote load and calculated G for the initial crack length a_0. Solve the crack growth da_1 from Eq. (12). There is always a unique solution if the R-curve is monotonically increasing. The next step is to calculate G for a crack length $a_0 + da_{i-1}$ and solve a new da_i. This process is repeated until convergence has been obtained or until the failure criterion has been satisfied. If the assumed remote load is below the residual strength this procedure will converge.

To solve the residual strength an additional iterative procedure is required. If convergence has been obtained the assumed remote load can be increased and the static growth can be solved again; if no convergence has been found, the assumed remote load should be decreased. With this in mind an iterative procedure can be built to solve the residual strength (e.g. bi-section method). This iterative procedure is probably not very efficient but it is suitable to solve the static growth of all tips. To do this G and da have to be replaced by the vectors containing the energy release rates (as determined with the Strip Yield model) and static growth of all crack tips.

Stiffened Panels

The effect of the stiffeners on the deformation behaviour of a panel is implemented by the displacement compatibility method, as described by Vlieger[13] and Swift[14]. This method is based on the concept that displacements at all rivets in the cracked panel should be equal to the corresponding displacements in the stiffeners. This approach was first applied in ARREST, a computer program developed at the NLR to predict the residual strength in stiffened panels with *one* crack.

Consider figure 3, where a panel configuration with two riveted stiffeners and a single central crack of length 2a is shown. The stiffener spacing is 2s. Each stiffener is fastened to the sheet by means of only one rivet at either side of the crack. The sheet is loaded at its ends by a uniform stress σ_R. Assuming equal displacements in sheet and stiffener at the panel ends, this implies a stiffener end stress of $\sigma_R E_{st}/E_{sh}$, where E_{sh} and E_{st} are the Young's moduli of sheet and stiffener, respectively. Owing to the presence of the crack, in the cracked region load will be transferred via the rivets from the sheet to the stiffener. To determine the displacements in sheet and stiffener at the rivet locations owing to the external stress σ_R and the interacting rivet forces F, the stiffened structure is split up into its components as depicted in the central part of figure 3. The displacements in sheet and stiffener are denoted by v_{sh} and v_{st}, respectively. The displacement in the cracked sheet is composed of the separate components as indicated

in the bottom part of figure 3, *i.e.* the displacement due to the remote stresses σ_R (v_a, see sketch a) and the displacement due to the rivet forces. The latter displacement is determined by considering this load case as a superposition of two load cases *i.e.* the case of a sheet with rivet forces but no crack (displacement v_b, see sketch b) and that of a sheet with a crack loaded along its edges by a stress distribution p(x) (displacement v_c, see sketch c). The stress distribution p(x) is equal in magnitude but of opposite sign to the stresses along the crack segment caused by the rivet forces in the uncracked sheet of sketch b, and serves to provide the necessary stress-free crack surface.
The displacements of the stiffener rivet points are composed of the displacements due to the end stress $\sigma_R E_{st}/E_{sh}$ and the displacements due to the rivet forces F. The rivet flexibility is included by means of an empirical relation proposed by Swift[15]. Due to this rivet flexibility there is a certain displacement of the rivets, v_{riv}, and the compatibility relation becomes:

$$v_{sh} = v_{st} - v_{riv} \tag{14}$$

Link-up criterion
As mentioned in the introduction, models reported in the literature differ in definitions and criteria for crack growth and link-up. Swift[2] first proposed the link-up or plastic zone touch criterion. This criterion implies that a ligament will fail if the sum of the sizes of the two plastic zones of two crack tips equals the ligament size. This method has also been adopted by Broek *et al.*[5] and De Wit *et al.*[6], who determined the plastic zone with the Dugdale equation[9]. Broek *et al.*[5] also applied a modified link-up criterion by including the effect of stable tearing, which reduces the distance between cracks and increases the stress intensity factors. This modification increased the accuracy of the model predictions. Smith *et al.*[7] modified the link-up model empirically to improve the accuracy of the model fit to the test data. Nilsson *et al.*[8] defined link-up as actual crack impingement of the leading crack and an MSD crack. A two-parameter crack growth criterion based on a constant near-tip opening profile leads to crack growth resistance when used in conjunction with the Dugdale model. Onset of crack growth is determined by a critical crack opening, whereas continuous growth is governed by a constant crack-opening angle. The NLR model presented here also defines link-up as actual crack impingement of the leading crack and an MSD crack. However, now the R-curve concept is used to assess the residual strength, see the previous two sub-sections.

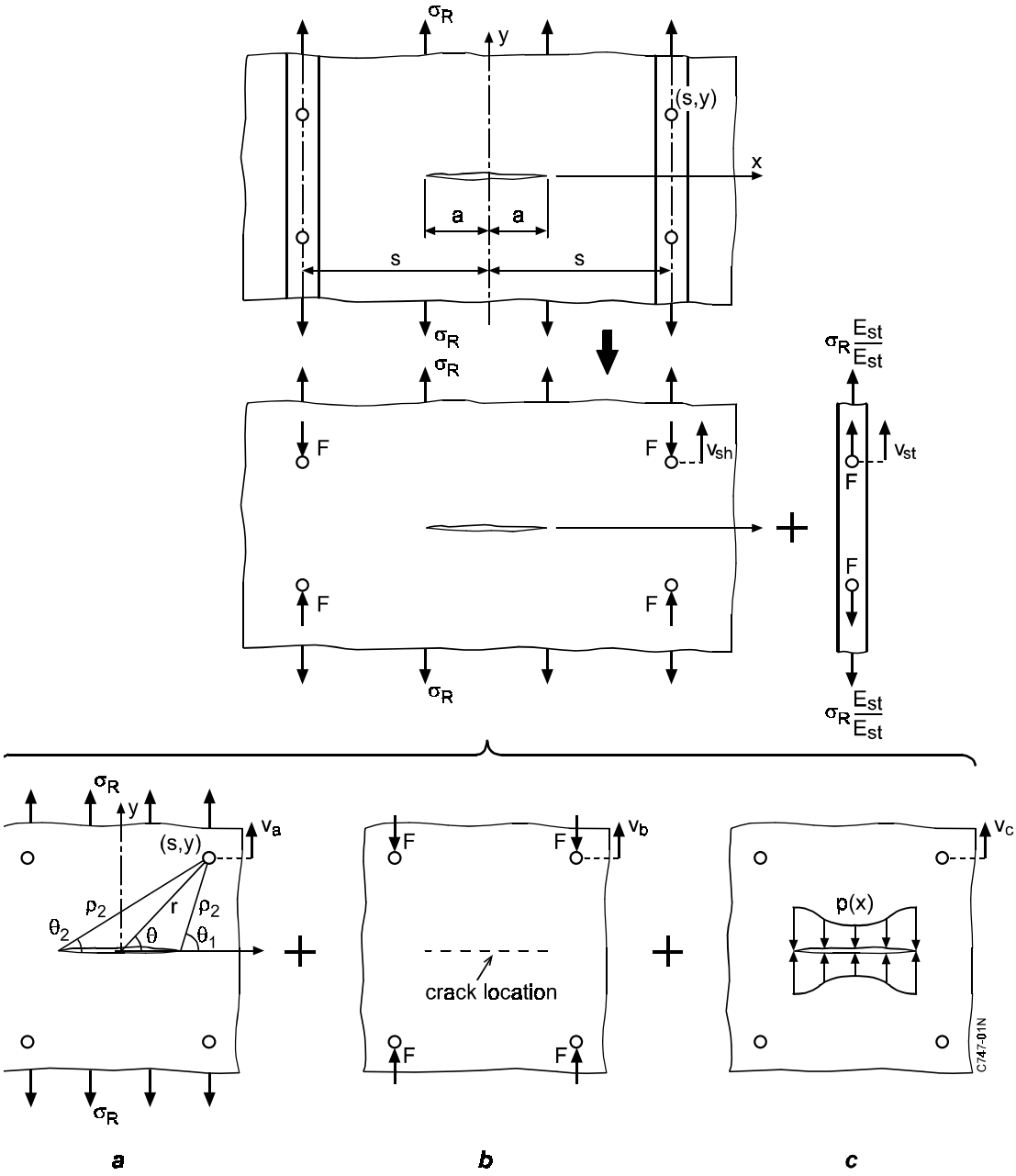

Figure 3 *Split-up of cracked stiffened panel into its components*

EXPERIMENTAL

Test description

The developed model is verified using experimental data from NLR, Foster-Miller and NIST. All panels were made from 2024-T3 aluminium panels without a lap joint. The NLR and Foster-Miller panels were provided with an Alclad layer, while NIST used bare panels. NLR panels 4 to 14 were stiffened with 7075-T6 strips spaced every 340

mm. NLR4 to NLR9 consisted of a skin crack extending between two stiffeners, NLR10 consisted of a skin crack extending under an intact stiffener, and NLR11 to NLR14 consisted of a skin crack extending under a broken stiffener. The Foster-Miller and NIST panels were unstiffened. Table 1 gives the geometry of the panels and the MSD configuration, with parameters defined in figure 4. All tests were done under displacement control and provided with anti-buckling guides to avoid out-of-plane deflection. More details of the tests can be found in ref [3,4] for the NLR tests (except for the first three tests, which are not described in the open literature), ref [5] for the Foster-Miller tests, and ref [6] for the NIST tests.

R-curve

The R-curve used for the model predictions was derived from the a-N data of the NLR04 test. It was not determined according to ASTM specification E561-86, but with the model itself by calculating for each stress step the corresponding point on the G-curve. In this way an R-curve is obtained including all model features and assumptions involved. This R-curve differs from the R-curve obtained from the ASTM specification and the relation between the two R-curves is currently under investigation.

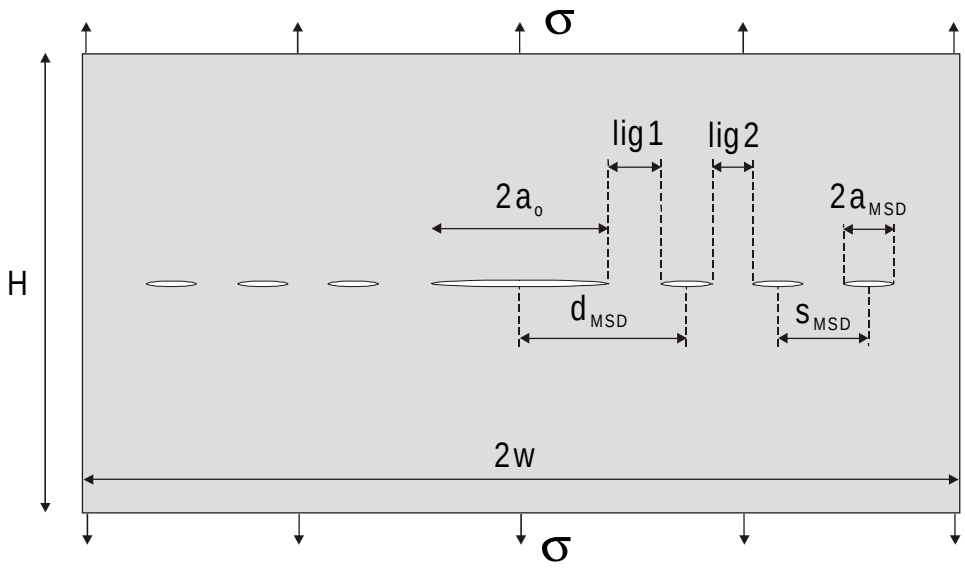

Figure 4 *Description of geometry parameters for flat MSD panels*

Table 1 *Panel geometry and MSD crack configuration with parameters defined in figure 4*

Panel	2W [mm]	t [mm]	H [m]	a_0 [mm]	d_{MSD} [mm]	$2a_{MSD}$ [mm]	lig1 [mm]	s_{MSD} [mm]	lig2 [mm]	# cracks per side
NLR1	304	1.21	0.7	49.86	–	–	–	–	–	–
NLR2	304	1.21	0.7	50.03	69.45	13.20	12.82	–	–	1
NLR3	304	1.21	0.7	24.90	44.41	11.94	13.50	26.31	14.37	2
NLR4	1190	1.27	1.83	75.0	–	–	–	–	–	–
NLR5	1190	1.27	1.83	85.0	–	–	–	–	–	–
NLR6	1190	1.27	1.83	60.1	–	–	–	–	–	–
NLR7	1190	1.27	1.83	60.0	115.3	25.0	42.8	–	–	1
NLR8	1190	1.27	1.83	60.5	225.7	25.1	152.7	–	–	1
NLR9	1190	1.27	1.83	60.0	115.4	25.1	42.9	109.1	84.0	2
NLR10	1190	1.27	1.83	150.1	–	–	–	–	–	–
NLR11	1190	1.27	1.83	150.1	–	–	–	–	–	–
NLR12	1190	1.27	1.83	80.3	–	–	–	–	–	–
NLR13	1190	1.27	1.83	80.3	199.3	25.2	106.4	–	–	1
NLR14	1190	1.27	1.83	80.0	176.6	25.1	84.1	118.2	93.1	2
FM1	508	1.016	1	50.8	–	–	–	–	–	–
FM2	508	1.016	1	88.9	–	–	–	–	–	–
FM3	508	1.016	1	134.2	–	–	–	–	–	–
FM4	508	1.016	1	76.2	114.3	12.7	31.8	–	–	1
FM5	508	1.016	1	91.4	114.3	12.7	16.6	–	–	1
FM6	508	1.016	1	96.5	114.3	12.7	11.5	38.1	25.4	2
FM7	508	1.016	1	94.0	114.3	12.7	14.0	38.1	25.4	3
FM8	508	1.016	1	101.6	114.3	7.6	8.9	25.4	17.8	2
FM9	508	1.016	1	40.7	63.5	20.3	12.6	50.8	30.5	2
FM10	508	1.016	1	40.7	63.5	12.7	16.5	38.1	25.4	2
FM11	508	1.016	1	63.5	88.9	25.4	12.7	50.8	25.4	2
FM12	508	1.016	1	38.1	88.9	25.4	38.1			1
NIST1	2286	1.016	3.988	177.8	–	–	–	–	–	–
NIST2	2286	1.016	3.988	101.6	–	–	–	–	–	–
NIST3	2286	1.016	3.988	254.0	–	–	–	–	–	–
NIST4	2286	1.016	3.988	177.8	190.5	10.2	7.6	25.4	15.2	3
NIST5	2286	1.016	3.988	71.1	88.9	15.2	10.2	38.1	22.9	3
NIST7	2286	1.016	3.988	254.0	266.7	12.7	6.3	38.1	25.4	5
NIST8	2286	1.016	3.988	241.3	266.7	12.7	19.1	38.1	25.4	10
NIST9	2286	1.016	3.988	127.0	165.1	10.2	33.0	25.4	15.2	10
NIST10	2286	1.016	3.988	254.0	266.7	12.7	6.3	38.1	25.4	5

Notes

- NLR 1 to NLR 3, all FM, all NIST: unstiffened
- NLR 4 to NLR 9 : skin crack extending between two stiffeners
- NLR 10 : skin crack extending under an intact stiffener
- NLR 11 to NLR 14 : skin crack extending under a broken stiffener

RESULTS AND DISCUSSION

Model

All predictions were made with the flow stress, σ_Y, instead of the yield strength, σ_{YS}. The flow stress is defined as the average between the yield strength and the ultimate tensile strength, UTS:

$$\sigma_Y = \frac{(\sigma_{YS} + UTS)}{2} \tag{14}$$

This was done since the model assumes linear elastic / ideal plastic material behaviour while 2024-T3 shows strain hardening. Previous experiments at the NLR[4] showed that for 2024-T3 Eq. (14) results in σ_Y = 424 MPa[1].

The calculation time on a Pentium III with a 733 MHz processor varied from a few seconds for an unstiffened panel with a leading crack only, to 14 minutes for a stiffened panel with two secondary cracks on both sides of a leading crack (NLR09) and 16 minutes for an unstiffened panel with 10 secondary cracks on both sides of a leading crack (NIST09).

Link-up and residual strength

Figures 5 to 7 give the comparisons between model prediction and experimental results from the NLR, Foster-Miller and NIST tests. There is fair agreement between the predicted values and the experimental values. It is seen that for a panel with a leading crack only (NLR01, 04-06, 10-12; FM01-03; NIST01-03) the prediction for the failure stress is in general too high: the reason for this is presently unknown. Since there are no further general trends in the deviation between model and experiment it is hard to explain the differences from a modelling point of view. One should consider the possibility of inaccuracies in the experimental results, since for all but one test there are no duplicates. The only duplicate tests carried out were NIST07 and NIST10. The differences between these two tests on identical panels are rather large: 18% for first link-up, 44% for second link-up and 32% for panel failure. Hence the observed deviation of the predictions from the experimental results lie within the experimental variation. Also, the observed deviations are similar to those found by Broek *et al.*[5], De Wit *et al.*[6], and Nilsson[8]. Smith *et al.*[7] obtained somewhat better predictions, but not before they fitted their model to the experimental results, *i.e.* they used a semi-empirical model. It should be noted that a better validation of the model would require more duplicate tests with the same MSD configuration, i.e. a statistically more reliable experimental result.

[1] This value of σ_Y would seem too high for 2024-T3. However it was obtained from the same batch of material used for the R-curve test, so it was adopted for all analyses.

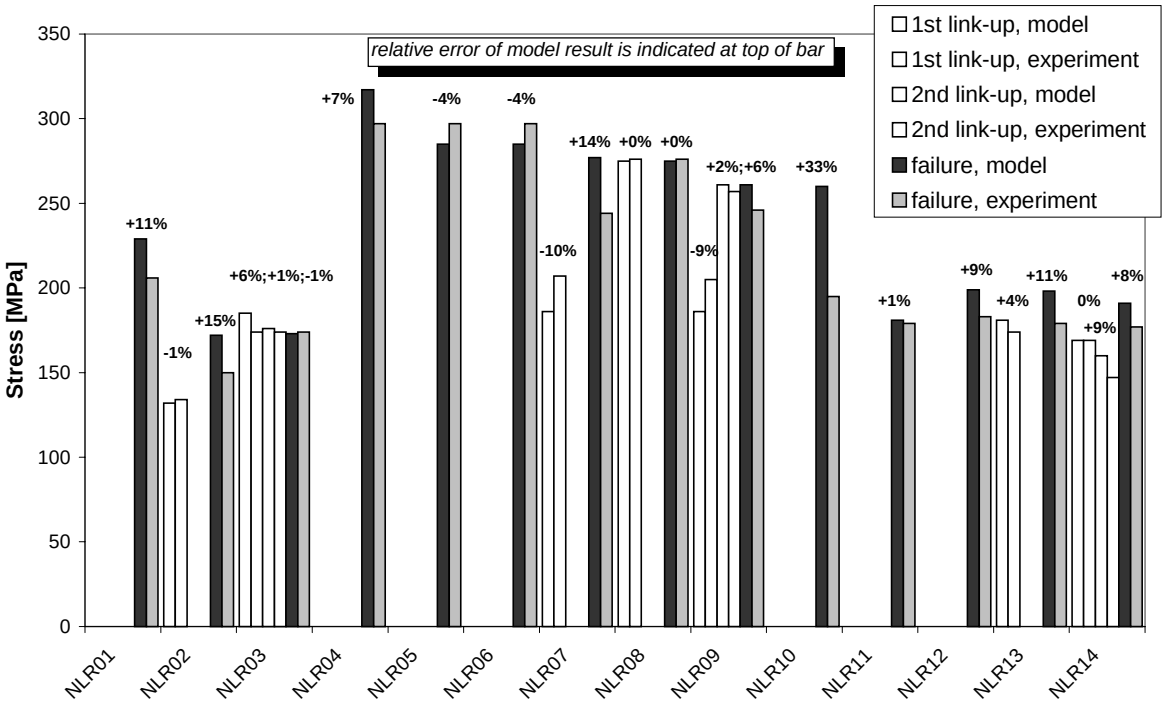

Figure 5 *Predicted and measured stress levels for link-up and failure for the NLR MSD panels. The relative deviation of the predictions from the experimental values is given at the top of each bar*

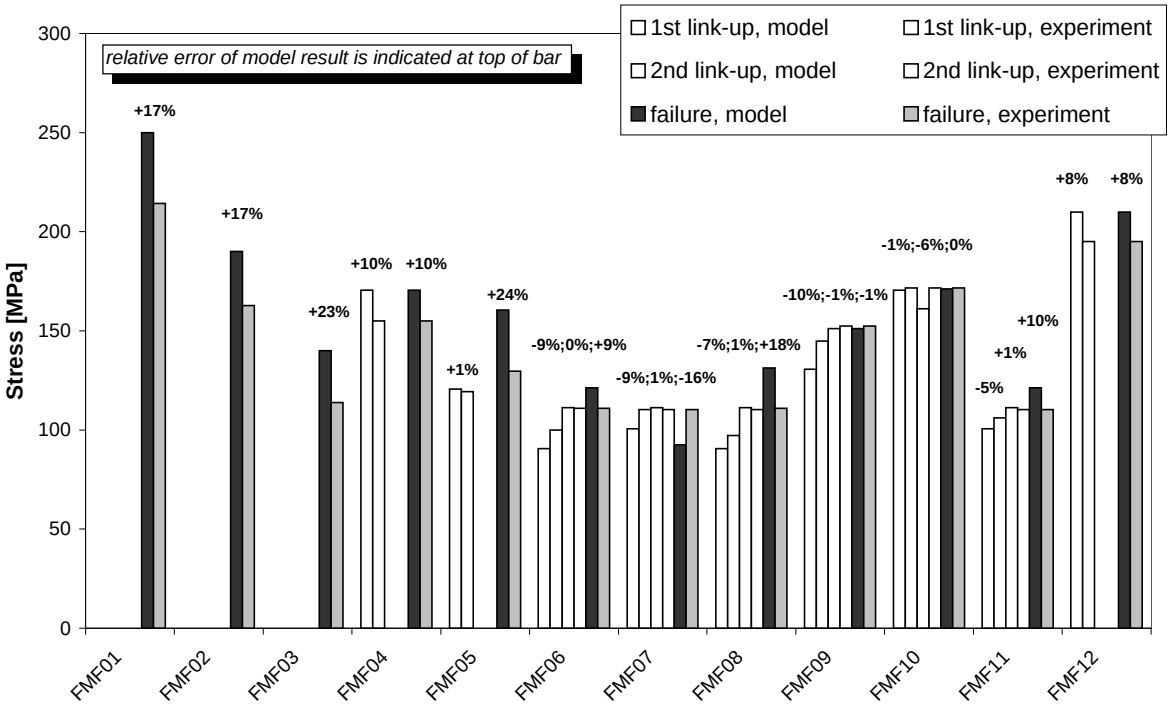

Figure 6 *Predicted and measured stress levels for link-up and failure for the Foster-Miller MSD panels. The relative deviation of the predictions from the experimental values is given at the top of each bar.*

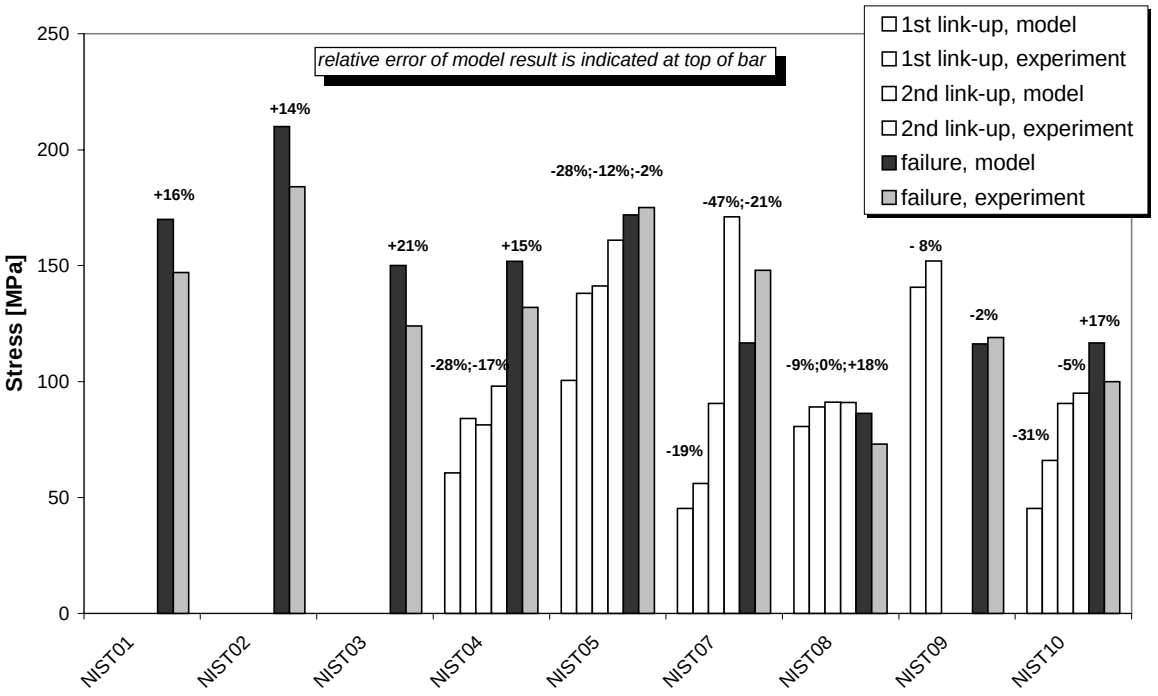

Figure 7 *Predicted and measured stress levels for link-up and failure for the NIST MSD panels. The relative deviation of the predictions from the experimental values is given at the top of each bar*

Crack growth

During the NLR tests static crack growth was observed in all panels. Crack length data were obtained as a function of the applied load. This enables us to verify the entire crack growth and link-up process predicted by the model. The experimental results are reported by Hoeve *et al.*[4]. Figures 8 and 9 give two representative examples for stiffened panels (NLR09 and NLR14).

It is seen that the crack growth process is predicted fairly well, especially during the link-up phase. Crack growth just before failure deviated from the measured values. The reason for this can be found in the application of the R-curve approach. Since the R-curve is based on a residual strength experiment with a panel of limited width (NLR04), the R-curve becomes unreliable for large crack lengths, *i.e.* just before failure.

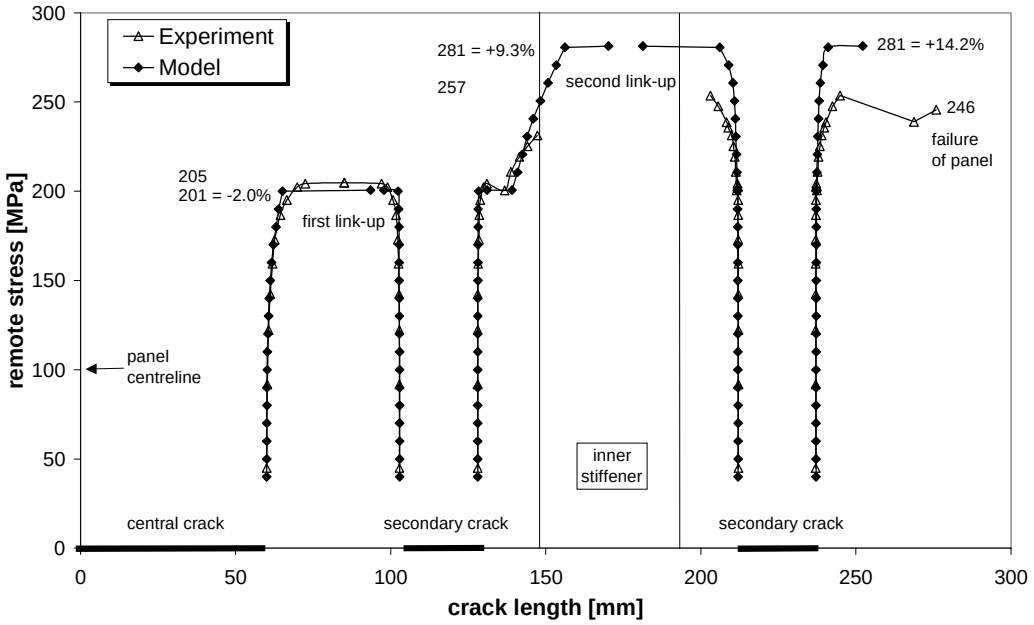

Figure 8 *Predicted and measured crack growth as a function of the applied remote stress for the NLR09 panel. The relative deviations of the predictions from the experimental values are indicated.*

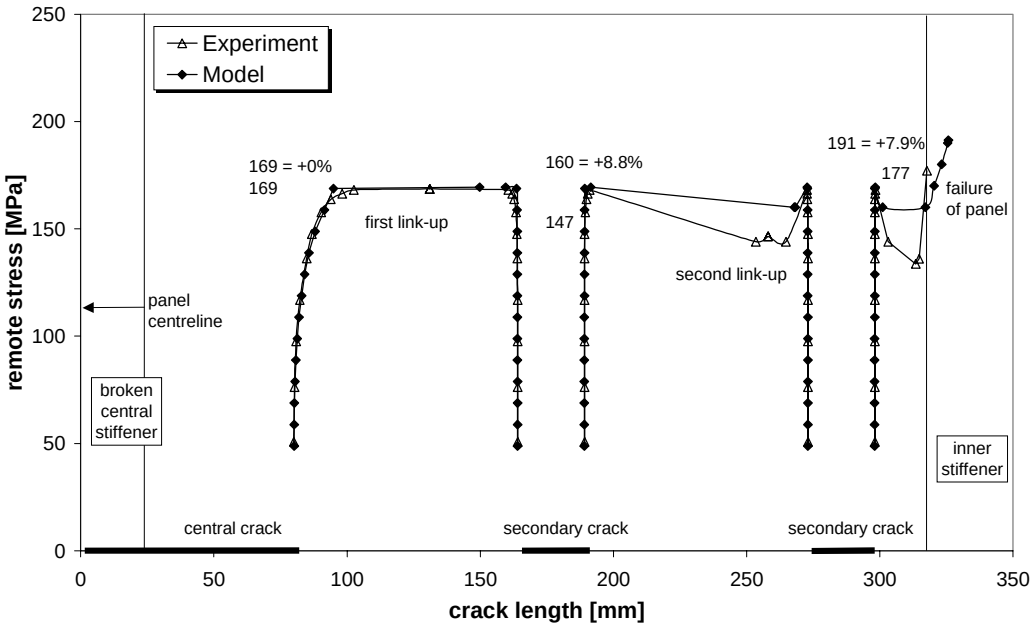

Figure 9 *Predicted and measured crack growth as a function of the applied remote stress for the NLR14 panel. The relative deviations of the predictions from the experimental values are indicated.*

CONCLUSIONS

An advanced engineering model to predict link-up and the residual strength in flat unstiffened and stiffened panels with one leading crack and MSD cracks is presented. This model is based on the Strip Yield model for calculation of the J-integral at all crack tips and the R-curve approach. The influence of stiffeners is modelled using the displacement compatibility method. Link-up was defined as actual crack impingement. From model verification with experimental results from different institutes the following conclusions are drawn:

- The predicted link-up loads and residual strengths agree fairly well with the experimental values.
- The observed deviations fall within the experimental errors reported in the literature. However, it is recommended to do more duplicate tests in the future, in order to obtain statistically reliable test results.
- The R-curve approach in combination with actual crack impingement as link-up criterion results in good predictions for the link-up stresses and the crack growth during the link-up phase.
- The predictions for residual strength and crack growth just before failure deviate from the measured values owing to unreliability of the R-curve for long cracks: the R-curve should actually be based on a wider panel.
- The relation between the R-curve used in the present model and the standard ASTM R-curve needs to be investigated in order to make the model of practical use for the industry.

REFERENCES

1. Schijve, J.; “Multiple-Site Damage in Aircraft Fuselage Structures,” *Fatigue Fract. Engng. Mater. Struct.*, Vol. 18, 1995, pp. 329-344
2. Swift, T.; “Widespread Fatigue Damage Monitoring – Issues and Concerns,” In: *Proc. 5th Int. Conf. on Structural Airworthiness of New and Ageing Aircraft*, 1993, pp. 113-150
3. Hoeve, ten, H.J.; Ottens, H.H.; Schra, L.; Vlieger, H.; “Residual Strength of Stiffened Panels With Multiple Site Damage,” in: *Proc. 7th Int. Fatigue Congress*, X.R. Wu and Z.G. Wang, Eds., Vol. 4, Higher Education Press, Beijing, China, 1999, pp. 2515-2520
4. Hoeve, ten, H.J.; Schra, L.; Michielsen, A.L.P.J.; Vlieger, H.; *Residual Strength Tests on Stiffened Panels With Multiple Site Damage*, NLR-CR-96792 L, National Aerospace Laboratory, Amsterdam, The Netherlands, 1996
5. Broek, D.; Jeong, D.Y.; Thomson, D.; “Testing and Analysis of Flat and Curved Panels with Multiple Cracks,” In: *Proc. FAA/NASA Int. Symp. Advanced Structural Integrity Methods for Airframe Durability and Damage Tolerance*, NASA Conference Publication 3274, 1994, pp. 85-98
6. De Wit, R.; Fields, R.J.; Low III, S.R.; Harne, D.E.; Foecke, T.; *Fracture Testing of Large Scale Thin-Sheet Aluminum Alloy*, National Inst. of Standards and Technology, NISTIR 5661, Gaithersburg, MD, USA, 1995

7. Smith, B.L.; Saville, P.A.; Mouak, A.; Myose, R.Y.; “Strength of 2024-T3 Aluminum Panels with Multiple Site Damage,” *Journal of Aircraft*, Vol. 37, No. 2, 2000, pp. 325-331
8. Nilsson, K.F.; “Elasto-Plastic Models for Interaction between a Major Crack and Multiple Small Cracks,” in: *Proc. FAA/NASA Symposium on Continued Airworthiness of Aircraft Structures*, 1996, Atlanta
9. Dugdale, D.S.; “Yielding of Steel Plates Containing Slits,” *Journal of the Mechanics and Physics of Solids*, Vol. 8, 1960, pp. 100-108
10. Tada, H.; Paris, P.C.; Irwin, G.R.; *The Stress Analysis of Cracks Handbook*, Del Research Corporation, St. Louis, MO, USA, 1973
11. Brice, J.R.; “Plastic Yielding at a Crack Tip,” in: *Proc. First Int. Conf. on Fracture*, Vol. 1, T. Yokobori, T. Kawasaki and J.L. Swedlow, Eds., The Japanese Society for Strength and Fracture of Materials, 1966, pp. 283-308
12. Ewalds, H.L.; Wanhill, R.J.H.; *Fracture Mechanics*, Edward Arnold Ltd, London, UK / Delftse Uitgevers Maatschappij b.v., Delft, The Netherlands, 1984
13. Vlieger, H.; Sanderse, A.; User’s manual of arrest, a computer routine for prediction of residual strength of cracked stiffened panels, NLR TR 75129 C, National Aerospace Laboratory NLR, Amsterdam, The Netherlands, 1975.
14. Swift, T.; “Fracture Analysis of Stiffened Structure,” *Damage Tolerance of Metallic Structures: Analysis Methods and Applications,* ASTM STP 842, J.B. Chang and J.L. Rudd, Eds., American Society for Testing and Materials, 1984, pp. 69-107
15. Swift, T.; “Development of the Fail-Safe Design Features of the DC-10,” *Damage Tolerance in Aircraft Structures, ASTM STP 486,* ASTM, Philadelphia, PA, USA, 1971, pp. 164-214